Arch. Metall. Mater. **63** (2018), 4, 1743-1748

DOI: 10.24425/amm.2018.125100

P. KAWULOK*#, P. PODOLINSKÝ**, P. KAJZAR**, I. SCHINDLER*, R. KAWULOK*, V. ŠEVČÁK*, P. OPĚLA*

THE INFLUENCE OF DEFORMATION AND AUSTENITIZATION TEMPERATURE ON THE KINETICS OF PHASE TRANSFORMATIONS DURING COOLING OF HIGH-CARBON STEEL

The aim of the performed experiments was to determine the influence of deformation and of austenitization temperature on the kinetics of phase transformations during cooling of high-carbon steel (0.728 wt. % C). The CCT and DCCT diagrams for austenitization temperature 940°C and DCCT diagram for austenitization temperature 1000°C were constructed with the use of dilatometric tests. On the basis of obtained results, a featureless effect of austenitization temperature and deformation on the kinetics of phase transformations during cooling of investigated steel was observed. Critical cooling rates for the transformation of martensite in microstructure fluctuated from 5 to 7°C·s^{-1} (depending on the parameters of austenitization and deformation), but only at cooling rates higher than 8°C·s^{-1} a dominant share of martensite was observed in the investigated steel, which resulted in the significant increase of hardness.

Keywords: High-carbon steel, cooling, transformation diagrams, microstructure, hardness.

1. Introduction

Phase transformations, which occur while cooling, and their products, respectively incurred structural phases (cementite, ferrite, pearlite, bainite, martensite) significantly affect the final steel properties. The influence of the cooling rate to the austenite transformation, respectively to the origination of the final structural phases, is expressed by the transformation diagrams. Transformation diagrams of anisothermal decomposition of austenite, whose validity is determined by the chemical composition and austenitization conditions (mainly temperature and dwell time) can be used for the optimization of cooling conditions of the given steel during its thermomechanical processing. These diagrams express the influence of the applied cooling rate to the phase transformation temperatures, the final microstructure and the hardness of steels as well. There are transformation diagrams of anisothermal decomposition of austenite without influence of deformation – continuous cooling transformation (CCT) diagrams or with influence of the previous deformation – deformation continuous cooling transformation (DCCT) diagrams [1-6].

Basic methods of determination of the phase transformations at steel heating or cooling are based, first of all, on measurement of changes of the physical features invoked by the phase transformation. The mostly used method for the physical determination of temperatures of the phase transformations is dilatometry, which is performed on specialized devices – dilatometers [7-9], or it is possible to use for these purposes also universal plastometers of Gleeble type [3,5,10]. Another physical method which can be used for determination of temperatures of the phase transformations is a differential thermal analysis [11,12]. In addition, it is also possible to use of specialized computer programs for the phase transformations determination, such as, for example, JMatPro [13,14], QTSteel [5,11] and IDS [15], which enable relatively quick and simple design of the transformation diagrams on the basis of a chemical composition, austenitization conditions and cooling rates of the investigated steels. Another possibility of designing the transformation diagrams is the use of artificial neural networks [16,17]. However, transformation diagrams designed by means of specialized software programs are, in some cases related especially to the austenite transformation affected by the prior deformation, significantly different from those designed with help of the dilatometric analysis [5,18]. From this point of view, the physical methods of the measurement of the phase transformation temperatures are irreplaceable.

The aim of this work was to determine the influence of deformation and of temperature of austenitization to the kinetics of the phase transformations during cooling of high-carbon steel (0.728 wt. % C).

2. Experiment description

Three sets of dilatometric tests were carried out with the use of the Gleeble 3800 plastometer with the integrated opti-

* VSB-TECHNICAL UNIVERSITY OF OSTRAVA, FACULTY OF METALLURGY AND MATERIALS ENGINEERING, 17. LISTOPADU 15/2172, 708 33 OSTRAVA – PORUBA, CZECH REPUBLIC
** TŘINECKÉ ŽELEZÁRNY, A.S., PRŮMYSLOVÁ 1000, 739 61 TŘINEC, CZECH REPUBLIC
# Corresponding author: petr.kawulok@vsb.cz

cal contactless dilatometer. For these purposes, cylindrical specimens of the examined steel with a diameter of 6 mm and length of 86 mm were prepared. In the middle of the length of the tested specimens, thermocouple wires were welded on the surface, which enable measurement of temperature during the course of the dilatometric tests. Chemical composition of the investigated high-carbon steel was as follows (in wt. %): 0.728 C – 0.96 Mn – 0.329 Si – 0.024 P – 0.019 S – 0.06 Cr.

All prepared specimens were electrically heated by a resistance heater in the plastometer Gleeble 3800 with a heating rate of 10°C·s^{-1} to the chosen temperatures of austenitization with the consequential two-minute dwell time on this temperature. In case of the first set of the dilatometric tests without deformation, which were carried out in order to determine a CCT diagram of the assessed steel for the austenitization temperature 940°C, the specimens after dwelling on the austenitization temperature were cooled down with selected constant cooling rates from 0.5 to 20°C · s^{-1} to the temperature of 25°C. In case of the second and third set of the dilatometric tests, which were performed to determine a DCCT diagram of the investigated steel for the austenitization temperature 940°C, or 1000°C, the specimens after the two-minute dwelling on the austenitization temperature were deformed by compression with a strain e = 0.35 at the strain rate of 1 s^{-1}. Consequently, the deformed specimens were cooled down with the constant cooling rates from 0.5 to 20°C · s^{-1} to the temperature of 25°C.

The example of deformed and dilatometrically tested specimen is shown on the Fig. 1. The maximum diameter of deformed part of specimen was in dependence on the chosen cooling rate ranging from 7.31 mm (for cooling rate of 20°C · s^{-1}) up to 7.42 mm (for cooling rate of 0.5°C · s^{-1}).

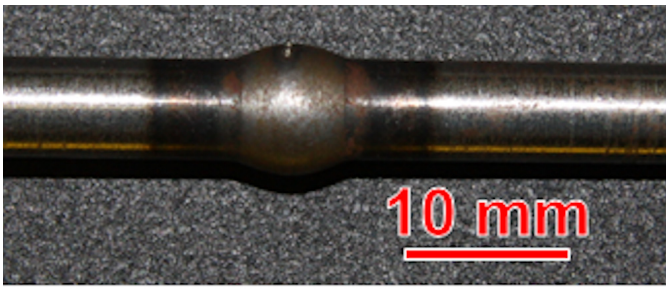

Fig. 1. The example of deformed and dilatometrically tested specimen

The selected dilatometrically tested specimens were cut transversely (in the place of welded thermocouple wires) and sequentially put to a metallographic analysis and hardness measurement. The prepared specimens were, to reveal their microstructure, chemically etched in Nital (4% solution of HNO_3 in ethanol) and subsequently metallographically analyzed by means of traditional optical microscopy with use of the Olympus GX 51. Hardness was measured by a Brinell method (HBW) with an exclusion of the decarburized surface layer of the specimens. A ball with a diameter of 2.5 mm were squeezed into the material with a force of 1839 N, whereas each specimen was tested three-fold and consequently there were determined an average value of its hardness.

3. Results and discussion

The dilatation curves, registered by an optical contactless dilatometer and representing a dependence of dilatation of individual specimens on temperature, were analyzed with the use of the special CCT software working in the Origin program environment. The determined temperatures and types of phase transformations were in the selected cases verified by the metallographic analyses and by the measurement of hardness on the transversal cut of the specimen, respectively. In this manner, there was determined a CCT and DCCT diagram for austenitization temperature of 940°C (see Fig. 2) and a DCCT diagram for austenitization temperature of 1000°C (see Fig. 3). In case of the DCCT diagram designed at the austenitization temperature of 940°C, there was not achieved the enclosure of the pearlite area, or there was not achieved the maximum cooling rate for the creation of pearlite by the performed dilatometric tests.

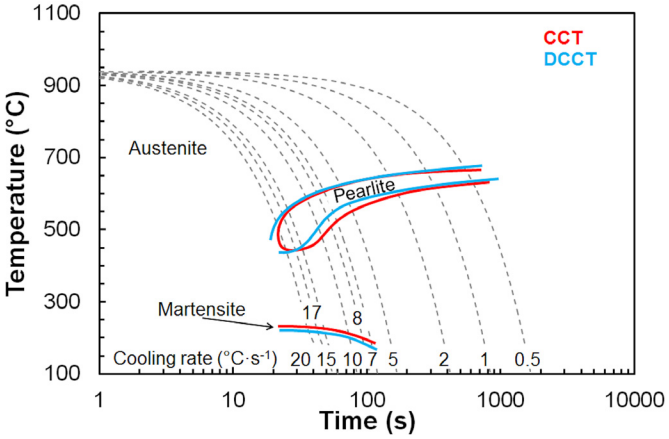

Fig. 2. Comparison of CCT and DCCT diagrams of investigated steel for austenitization temperature 940°C

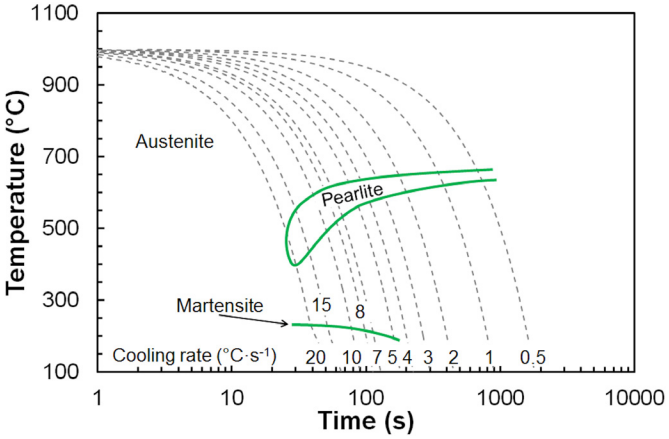

Fig. 3. DCCT diagram of investigated steel for austenitization temperature 1000°C

In case of austenitization temperature 940°C, the perlite area was lightly displaced to the left as a result of deformation, i.e. to the higher cooling rates, respectively to the shorter times. Under these experimental conditions, thus, the perlite area was

not enclosed. Neither the chosen austenitization temperatures nor the effect of the previous deformation significantly influenced the temperatures of the start of pearlite transformation. A certain small effect of the combination of deformation and austenitization temperature expressed itself by displacement of the start of temperature of the martensitic transformation – see Fig. 4. In case of austenitization of the specimens at temperature 940°C, deformation caused decreasing the temperature of the start of martensite transformation approximately by 10°C. It corresponds to the results published in the work [19,20] and the presumption that during deformation of austenite, a rich network of dislocations was originating which prevents from the progress of the phase boundary. It can be assumed that increasing austenitization temperature will lead to the increasing the initial austenitization grain size and, so, to the increasing the temperature of the start of the martensitic transformation [21,22]. However, due to deformation and recrystallization, the initial austenitization grain size should be decreased. A combination of austenitization and sequential deformation of high-carbon steel at temperature 1000°C, resulted in a displacement of the start of the martensitic transformation to temperatures, which are higher than in case of the non-deformed specimens austenitized at the temperature 940°C. In this regard, it seems that the effect of deformation to the size of the initial austenitization grain was in this case suppressed owing to the temperature of deformation.

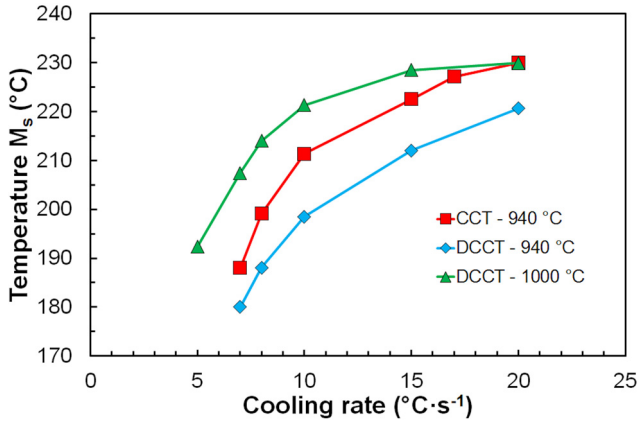

Fig. 4. The effect of deformation and austenitization temperature to the temperature of the start of martensitic transformation – M_s

Based on the transformation diagrams specified in Fig. 2 and Fig. 3, however, it is clear that the effect of the austenitization temperature or previous deformation was unequivocally overlapped owing to the cooling rate. At the cooling rates from 0.5 to 5°C·s^{-1} (in case of the specimens austenitized at the temperature 940°C), or up to 4°C·s^{-1} (in case of the specimens austenitized at the temperature 1000°C), the microstructure is created almost exclusively by pearlite, which completes a very small share of ferrite (about 1%) on the borders of the perlite blocks – see Fig. 5a, Fig. 6a, Fig. 7a and TABLE 1. This fact, among others, proves that the investigated steel is slightly hypoeutectoid. It is necessary to note that the ferrite transformation was not detected by the optical dilatometer due to the very small share of ferrite in the microstructure of specimens. In the microstructure of specimens which were cooled by the rate of 7°C·s^{-1} (in case of the dilatometric tests performed at the austenitization temperature 940°C) and by the rate of 5°C·s^{-1} (in case of the dilatometric tests performed at the austenitization temperature of 1000°C) a very low share of martensite was detected – see Fig. 5b, Fig. 6b, Fig. 7b and Table 1. Higher cooling rates resulted in achieving

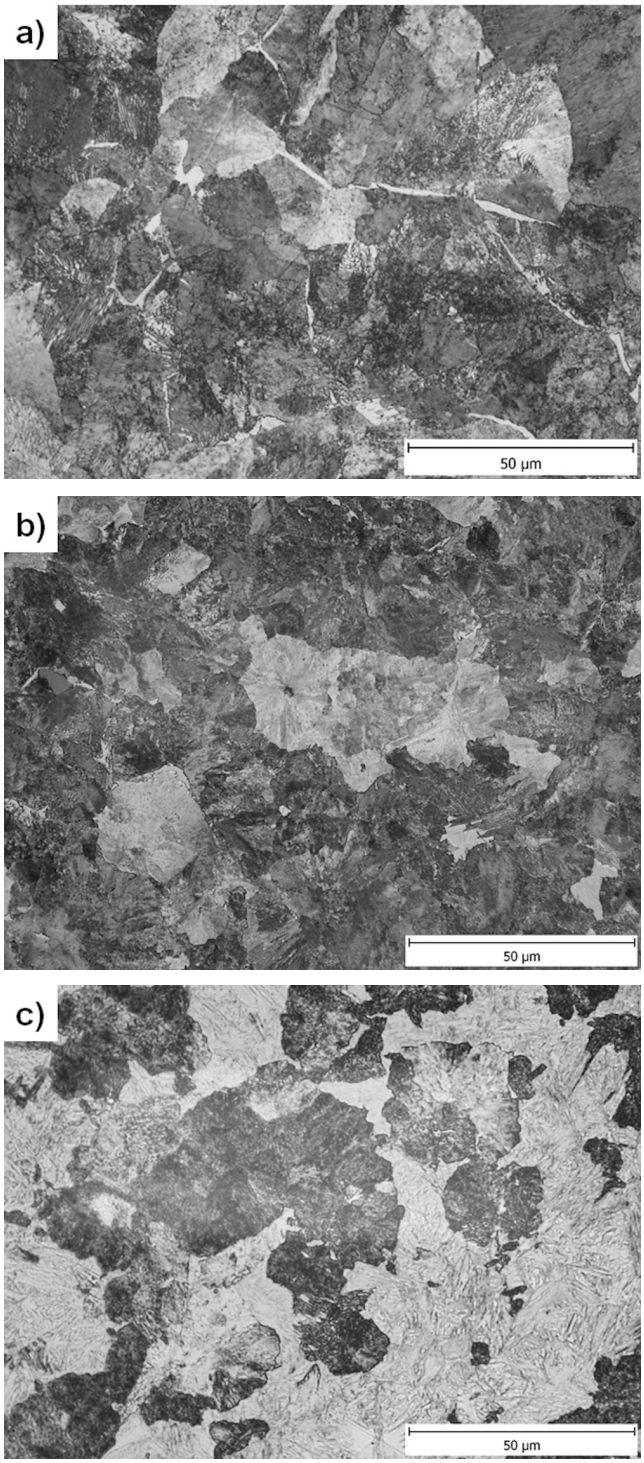

Fig. 5. The microstructure of the dilatometrically tested specimens which were austenitized at the temperature 940°C and cooled down by the selected cooling rates without the influence of previous deformation: a) cooling rate of 0.5°C·s^{-1}; b) cooling rate of 7°C·s^{-1}; c) cooling rate of 15°C·s^{-1}

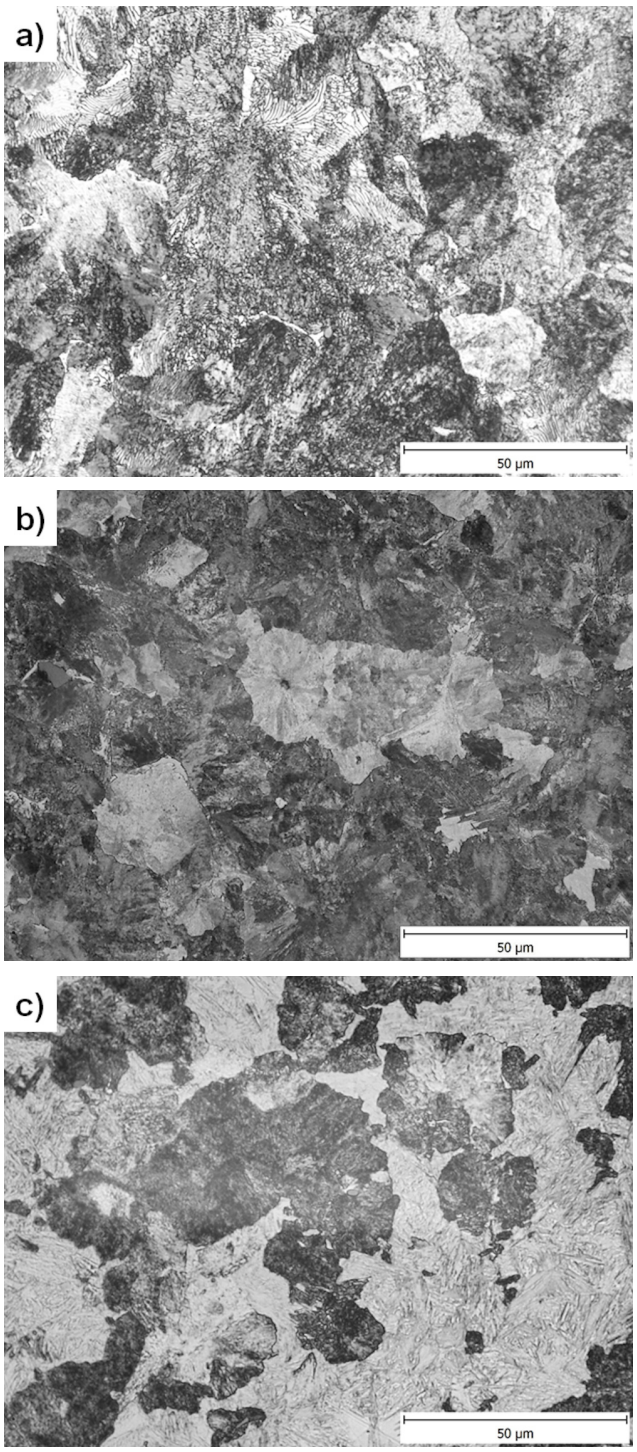

Fig. 6. The microstructure of the dilatometrically tested specimens which were austenitized and deformed at the temperature 940°C and cooled down by the selected cooling rates: a) cooling rate of 0.5°C·s^{-1}; b) cooling rate of 7°C·s^{-1}; c) cooling rate of 15°C·s^{-1}

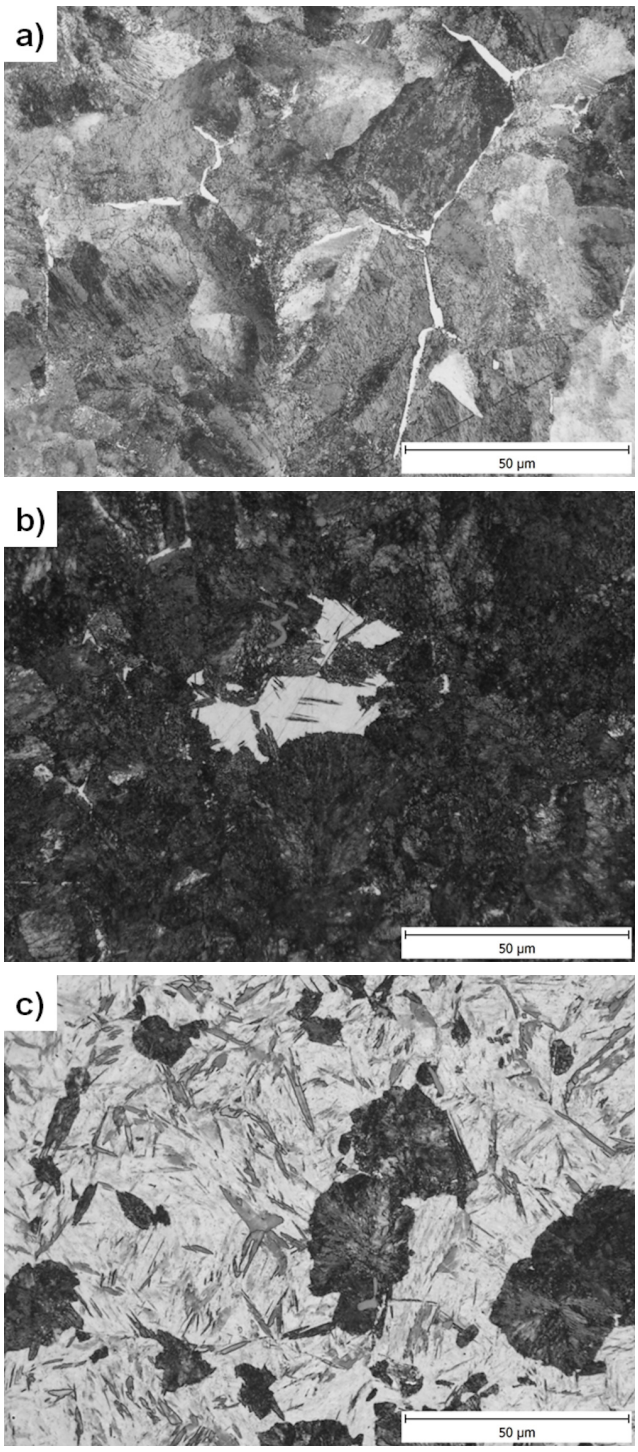

Fig. 7. The microstructure of the dilatometrically tested specimens which were austenitized and deformed at the temperature 1000°C and cooled down by the selected cooling rates: a) cooling rate of 0.5°C·s^{-1}; b) cooling rate of 5°C·s^{-1}; c) cooling rate of 15°C·s^{-1}

the microstructure consisting of the mixture of pearlite and martensite – see Fig. 5c, Fig. 6c, Fig. 7c and Table 1, whereas the share of pearlite in the microstructure was being decreased with the increasing of cooling rate – see Fig. 8.

The increase of the cooling rate resulted to gradual increasing the share of martensite in the microstructure of investigated steel. It consequently approved itself by the resulting hardness of the dilatometrically tested specimens, whereas a significant increase of hardness was reached at the cooling rates higher than 8°C·s^{-1} – see Fig. 9.

Based on the achieved results, it is clear (see Fig. 2, 3 and Table 1), that the critical cooling rate for the creation of martensite in the microstructure of the investigated steel is 7°C·s^{-1} (in case of specimens austenitized and deformed at the temperature 940°C), or 5°C·s^{-1} (in case of specimens austenitized and deformed at the temperature 1000°C), however the shares

TABLE 1

The share of structural phases (F – ferrite, P – pearlite, M – martensite) in dilatometry tested samples

Cooling rate	CCT – 940°C			DCCT – 940°C			DCCT – 1000°C		
	F	P	M	F	P	M	F	P	M
(°C·s^{-1})	(%)	(%)	(%)	(%)	(%)	(%)	(%)	(%)	(%)
0.5	1	99	—	1	99	—	1	99	—
2	1	99	—	1	99	—	1	99	—
4	not analyzed			not analyzed			1	99	—
5	not analyzed			not analyzed			—	97	3
7	—	95	5	1	96	3	not analyzed		
8	—	85	15	—	85	15	—	78	22
15	—	32	68	—	40	60	—	25	75
20	—	10	90	—	20	80	—	8	92

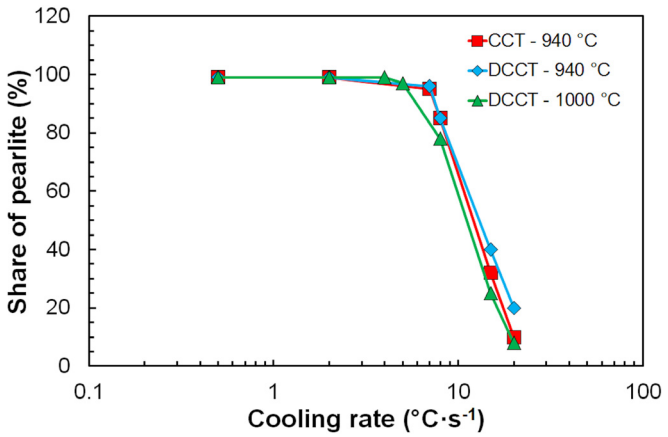

Fig. 8. Influence of the applied cooling rate to the share of pearlite in the microstructure

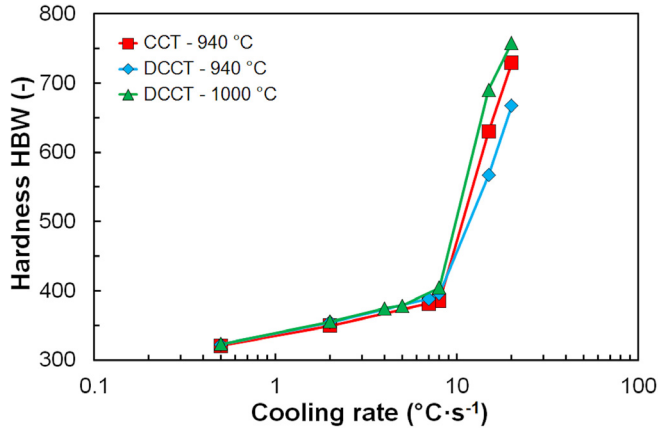

Fig. 9. Hardness of dilatometrically tested specimens

of martensite transformed at these cooling rates are very low. The critical cooling rate for the transformation of pearlite in the microstructure of the assessed steel was not precisely determined. Based on the achieved results, however, it can be assumed that in case of non-deformed specimens austenitized at the temperature 940°C and also specimens deformed and austenitized at the temperature 1000°C, the critical cooling rate for the transformation of pearlite will approach to 20°C·s^{-1}. However, in case of specimens austenitized and deformed at the temperature of 940°C, it is impossible to estimate this rate, because at the cooling rate of 20°C·s^{-1} the microstructure of the assessed specimen contained 20% of pearlite yet – see Table 1 and Fig. 10.

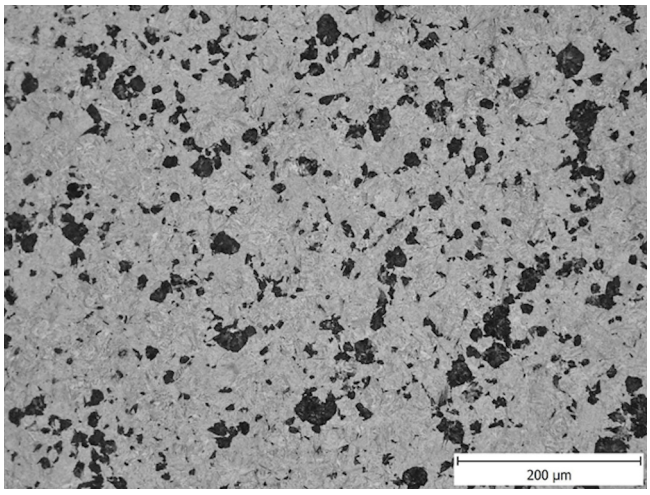

Fig. 10. Microstructure of specimen austenitized and deformed at the temperature 940°C and consequently cooled with the cooling rate of 20°C·s^{-1}

The work [20] examines an effect of deformation to the kinetics of the phase transformations during cooling of high-carbon steel with a similar chemical composition and similar parameters of austenitization (960°C) and deformation as in case of steel investigated by us. Steel used in the work [20] was slightly hypereutectoid (0.794 wt. % C) and, in addition, was alloyed by chromium (0.67 wt. % Cr). The comparison of the transformation diagrams defined by us (see Fig. 2 and 3) with the diagrams defined in the work [20] (see Fig. 11) produces interesting results.

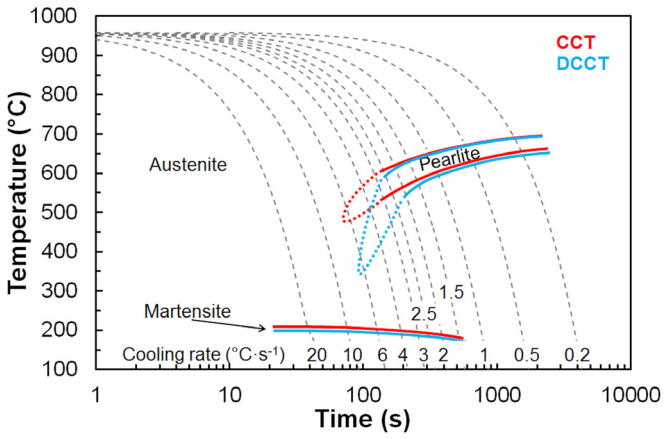

Fig. 11. Comparison of CCT a DCCT diagrams of the rail steel – class IH [20]

Lower austenitization temperature, shorten dwell time at this temperature, and lower content of chromium in our investigated steel, in comparison with steel used in the work [20], led to an increase the critical cooling rates for the formation of pearlite and martensite, which is corresponding to the results

presented in the works [23,24]. A lower content of carbon in our investigated steel resulted, in comparison with steel used in the work [20], in achieving the higher temperatures of the start of martensitic transformation.

4. Conclusions

By using the dilatometric analyses, which were completed by metallographic analyses and hardness measurement, transformation diagrams of CCT type (for the austenitization temperature 940°C) and DCCT type (for the austenitization temperature 940°C or 1000°C) of high-carbon steel with the content of carbon of 0.728 wt. % were constructed.

Based on the achieved results, it is possible to unequivocally claim that the effect of austenitization temperature (therefore the initial grain size) as well as the prior deformation is insignificant. Austenitization and deformation of the investigated steel at higher temperature resulted in only slight increasing the temperatures of the start of the martensitic transformation. From the point of view of structural processes, a cooling rate plays a key role. Critical cooling rates for the transformation of martensite fluctuated from 5 to 7°C · s^{-1} (dependent on parameters of austenitization and deformation), but only at cooling rates higher than 8°C · s^{-1} a higher share of martensite occurred in the investigated steel, which resulted in the significant increase of hardness.

By comparing the reached results with the results presented in the work [20] there was confirmed that higher austenitization temperature, longer dwell time at this temperature (therefore the higher austenitic grain size) together with a higher content of chromium in steel leads to a shift of the pearlitic nose to a smaller cooling rates and leads to a decrease of critical cooling rate for the transformation of martensite.

Acknowledgements

This paper was created at the Faculty of Metallurgy and Materials Engineering within the Project No. LO1203 "Regional Materials Science and Technology Centre - Feasibility Program" funded by the Ministry of Education, Youth and Sports of the Czech Republic; and within the students' grant project SP2018/105 supported at the VŠB – TU Ostrava by the Ministry of Education, Youth and Sports of the Czech Republic.

REFERENCES

[1] S. Zheng, Q. Wu, Q. Huang, S. Liu, Y. Han, Fusion Eng. Des. **86** (9-11), 2616-2619 (2011), DOI: 10.1016/j.fusengdes.2011.02.072.

[2] J. Trzaska, L.A. Dobrzański, J. Mater. Process. Tech. **192-193**, 504-510 (2007), DOI: 10.1016/j.jmatprotec.2007.04.099.

[3] W.J. Hui, N. Xiao, X.L. Zhao, Y.J. Zhang, Y.F. Wu, J. Iron Steel Res. Int. **24** (6), 641-648 (2017), DOI: 10.1016/S1006--706X(17)30096-1.

[4] F. Nürnberger, O. Grydin, M. Schaper, F.W. Bach, B. Koczurkiewicz, A. Milenin, Steel Res. Int. **81** (3), 224-233 (2010), DOI: 10.1002/srin.200900132.

[5] R. Kawulok, I. Schindler, P. Kawulok, S. Rusz, P. Opěla, Z. Solowski, K.M. Čmiel, Metalurgija. **54** (3), 473-476 (2015).

[6] F.R. Xiao, B. Liao, G.Y. Qiao, S.Z. Guan, Mater. Charact. **57** (4-5), 306-313 (2006), DOI: 10.1016/j.matchar.2006.02.003.

[7] B. Białobrzeska, R. Dziurka, A. Żak, P. Bała, Arch. Civ. Mech. Eng. **18** (2), 413-429 (2018), DOI: 10.1016/j.acme.2017.09.004.

[8] A. Grajcar, M. Opiela, Influence of plastic deformation on CCT-diagrams of low-carbon and medium-carbon TRIP-steels, J. Achiev. Mater. Manuf. Eng. **29** (1), 71-78 (2008).

[9] A. Pastor, P. Valles, I. Amurrio, S.F. Medina, Eng. Fail. Anal. **56**, 520-529 (2015), DOI: 10.1016/j.engfailanal.2014.11.016.

[10] R. Kawulok, I. Schindler, P. Kawulok, S. Rusz, P. Opěla, J. Kliber, Z. Solowski, K.M. Čmiel, P. Podolinsky, M. Mališ, Z. Vašek, F. Vančura, Metalurgija **55** (3), 357-360 (2016).

[11] M. Kawulokova, B. Smetana, S. Zla, A. Kalup, E. Mazancova, P. Váňova, P. Kawulok, J. Dobrovska, S. Rosypalova, J. Therm. Anal. Calorim. **127** (1), 423-429 (2017), DOI: 10.1007/s10973-016-5780-4.

[12] M. Gojic, M. Suceska, M. Rajic, J. Therm. Anal. Calorim. **75** (3), 947-956 (2004), DOI: 10.1023/B:JTAN.0000027188.58396.03.

[13] N. Saunders, Z. Guo, X. Li, A.P. Miodownik, J.P. Schille, JOM-J. Min. Met. Mat. S. **55** (12), 60-65 (2003), DOI: 10.1007/s11837-003-0013-2.

[14] Z.L. Guo, N. Saunders, A.P. Miodownik, J.P. Schille, Int. J. Metall. Eng. **2** (2), 198-202 (2013), DOI:10.5923/j.ijmee.20130202.11.

[15] J. Mittinen, Solidification analysis package for steels-user's manual of DOS version. University of Technology, Helsinki (1999).

[16] L.A. Dobrzański, J. Trzaska, J. Mater. Process. Tech. **157** (SI), 107-113 (2004), DOI: 10.1016/j.jmatprotec.2004.09.009.

[17] W. You, W.H. Xu, Y.X. Liu, B.Z. Bai, H.S. Fang, J. Iron Steel Res. Int. **14** (4), 39-42 (2007).

[18] L.A. Dobrzanski, J. Trzaska, Comp. Mater. Sci. **30** (3-4), 251-259 (2004), DOI: 10.1016/j.commatsci0.2004.02.011.

[19] J. Adamczyk, M. Opiela, J. Mater. Process. Tech. **157**, 456-461 (2004), DOI: 10.1016/j.jmatprotec.2004.07.148.

[20] R. Kawulok, I. Schindler, P. Kawulok, V. Kawulok, S. Rusz, P. Opěla, P. Podolinsky, V. Kurek, Study of kinetics phase transformations after plastic deformation of rail steel class IH alloyed with chromium, in: Metal 2016: 25th Anniversary International Conference on Metallurgy and Materials, 403-408 (2016).

[21] H.S. Yang, H.K.D.H. Bhadeshia, Scripta Mater. **60** (7), 493-495 (2009), DOI: 10.1016/j.scriptamat.2008.11.043.

[22] S. Turteltaub, A.S.J. Suiker, Int. J. Solids. Struct. **43** (24), 7322-7336 (2006), DOI: 10.1016/j.ijsolstr.2006.06.017.

[23] H. Hofmann, D. Mattissen, T.W. Schaumann, Steel Res. Int. **80** (1), 22-28 (2009), DOI: 10.2374/SRI08SP113.

[24] X.F. Li, P. Langenberg, S. Münstermann, W. Bleck, Recent developments of modern rail steels, in: The 5th International Conference on HSLA Steels, 775-782 (2005).